Cancer Biol Med 2018. doi: 10.20892/j.issn.2095-3941.2018.0016

ORIGINAL ARTICLE

OPEN ACCESS

Increased paracellular permeability of tumor-adjacent areas in 1,2-dimethylhydrazine-induced colon carcinogenesis in rats

Viktoria V. Bekusova[1], Evgeny L. Falchuk[1], Larisa S. Okorokova[1], Natalia M. Kruglova[1], Alexander D. Nozdrachev[1,2], Alexander G. Markov[1]

[1]Department of Physiology, St. Petersburg State University, St. Petersburg 197183, Russia; [2]I.P.Pavlov Institute of Physiology, Russian Academy of Sciences, St. Petersburg 199034, Russia

ABSTRACT

Objective: The morphology and functions of the proximal and distal large intestine are not the same. The incidence of colorectal cancer in these regions is also different, as tumors more often appear in the descending colon than in the ascending colon. Inflammatory bowel disease and colorectal cancer can increase transepithelial permeability, which is a sign of reduced intestinal barrier function. However, there is not enough evidence to establish a connection between the difference in colorectal cancer incidence in the proximal and distal colon and intestinal permeability or the effects of carcinogenesis on the barrier properties in various areas of the colon. The aim of the study was to assess the permeability of different segments of the large intestine according to a developed mapping methodology in healthy rats and rats with 1,2-dimethylhydrazine (DMH)-induced colon adenocarcinoma.

Methods: The short circuit current, the transepithelial electrical resistance and the paracellular permeability to fluorescein of large intestine wall of male Wistar rats were examined in the Ussing chambers. The optical density of the solution from the serosa side to assess the concentration of the diffused fluorescein from mucosa to serosa was analyzed by spectrophotometry. The morphometric and histological studies were performed by optical microscopy.

Results: Rats with DMH-induced colon adenocarcinomas showed elevated transepithelial electrical resistance in the areas of neoplasm development. In contrast, there was no change in the electrophysiological properties of tumor adjacent areas, however, the paracellular permeability of these areas to fluorescein was increased compared to the control rats and was characterized by sharply reduced barrier function.

Conclusions: The barrier properties of the colon vary depending on tumor location. The tumors were less permeable than the intact intestinal wall and probably have a negative influence on tumor-adjacent tissues by disrupting their barrier function.

KEYWORDS

Rat; 1,2-dimethylhydrazine; colorectal cancer; Ussing chamber; short circuit current; transepithelial electrical resistance; intestinal permeability

Introduction

The intestinal barrier is well defined, mainly due to the selective permeability of colonocyte membranes and the tight junctions between epithelial cells[1,2]. Pathophysiological processes, such as cancer, are associated with increased intestinal permeability and the destruction of intestinal barrier function[3-9]. Colorectal cancer (CRC) is among the most common types of cancer[10], and leakage of certain substances, such as proinflammatory cytokines[11-13] and epidermal growth factor[14], from the luminal compartment into the interstitium and vasculature, or vice versa, may play a role in tumorigenesis[8]. Some authors have suggested that tumor formation is associated with increased tight junction permeability[6-9]. Specific effects on tight junctions have been shown to be integral to bacterial invasion and tumor progression[15] and might be key in cancer metastasis[6]. Leakage has implications for both cancer progression and cancer detection, and possibly therapy[8]. Yet, the role of intestinal permeability in cancer pathogenesis has not been well investigated.

The incidence rates of CRC in the proximal and distal intestine are different, and CRC more commonly develops in the descending colon than in the ascending colon[16,17]. Studies

Correspondence to: Viktoria V. Bekusova
E-mail: v.bekusova@spbu.ru
Received January 23, 2018; accepted April 12, 2018.
Available at www.cancerbiomed.org

suggest that segments of the large intestine are significantly different in morphology and function, in particular how they absorb and secrete Na^+ and Cl^{-}[1, 18]. We hypothesized that the functional properties of the intestinal tissue might play an important role in tumor formation. However, there is not enough evidence to determine whether the functional properties of different parts of the large intestine change in the same or different ways during colon carcinogenesis and what effect tumorigenesis has on permeability.

The aim of the study was to assess the permeability of segments of the colon and rectum according to a developed mapping methodology and by analyzing electrophysiological parameters and paracellular permeability in healthy rats and rats with 1,2-dimethylhydrazine (DMH)-induced colon adenocarcinoma.

In this study, we showed that tumor tissues have different electrophysiological parameters than the tissues in healthy controls and probably create a specific microenvironment that negatively influences tumor-adjacent tissues by disrupting barrier function.

Materials and methods

Male Wistar rats aged 2 months weighing 150–180 g (n = 18) were housed in cages (5 rats in each cage) under a standard light/dark cycle (12 h light:12 h dark) at 22 ± 2 °C with *ad libitum* access to tap water and complete pelleted feed. The studies were carried out in accordance with the guidelines of the FELASA[19]. All chemicals were obtained from Sigma Aldrich (Taufkirchen, Germany).

Experimental model

Animals were randomly subdivided into 2 groups. The rats in the control group (n = 8) were not exposed to the carcinogen, whereas rats in the experimental group (n = 10) were administered 5 subcutaneous injections of DMH, weekly at 21 mg/kg of body weight (each dose). At this dosage, the carcinogen induces multiple colon tumors in most rats[20,21]. DMH was *ex tempore* dissolved in normal saline and neutralized with sodium bicarbonate (pH 7.0). All animals were weighed once a week.

To evaluate the permeability of the colon 6 months after the first carcinogen injection, the rats were decapitated with a guillotine (Open Science, Russia) without anesthesia, which can cause changes in permeability[22], autopsied by longitudinally opening the intestines on the mesenteric line, and washed with Krebs-Ringer solution. The position, number, and size of the tumors were recorded.

Mapping the intestinal segments

The large intestine of rats is divided into the following parts: the caecum; ascending, transverse, and descending colons; and the rectum. The overall length of the colon and rectum in Wistar rats aged 7–8 months, as previous experiments showed, varies from 16 to 24 cm. The rectum, which is 1/7 of the length of the colon, is 2–3 cm in length. To study intestinal permeability, we employed analogous segments of the colon and rectum, based on the relief of the intestinal mucosa. In the ascending colon, the folds are arranged at angles to each other, forming a herringbone structure, whereas in the descending colon, the folds are longitudinal and run parallel[20]. This approach allows us to obtain the most detailed scans of intestinal permeability in the proximal and distal colon.

We cut the large intestine of the rats into several segments (**Figure 1 a–h**), and the total number of control samples was 62, with 16 segments of ascending colon, 8 segments of transverse colon, 31 segments of descending colon, and 7 segments of the rectum.

Mapping of the colon segments in the experimental group of 1, 2-dimethylhydrazine-induced rats depended on the location of the developed neoplasms, and only approximately corresponded to the colon segments of the control group. To map the large intestine in the experimental group of rats, we used the following classifications: non-tumor, tumor, and tumor-adjacent. The tumor-adjacent segments were the two

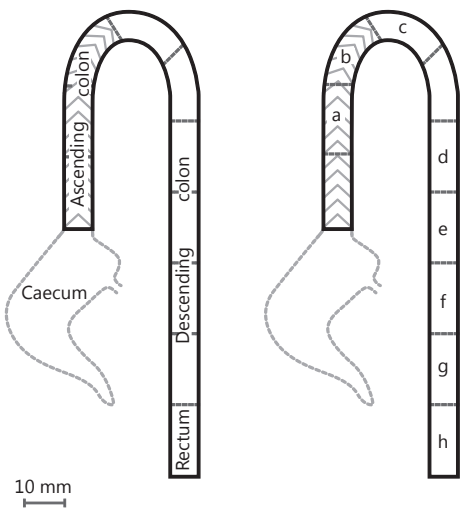

Figure 1 Mapping the segments of the large intestine (scheme). The large intestine is divided into several parts: the ascending, transverse, descending colon and rectum. (a) and (b) segments corresponding to the ascending colon, (c) to the transverse colon, (d, f, g, e) to the descending colon and (h) to the rectum.

segments from both sides of a tumor. The overall number of experimental samples was 72, with 16 tumor tissue samples, 27 tumor-adjacent tissue samples, and 29 non-tumor tissue samples.

Electrophysiological parameters of the large intestinal wall

The short circuit current and transepithelial electrical resistance of the large intestine wall were studied according to a previously described protocol[23]. Briefly, segments of the large intestine were mounted in Ussing chambers filled with Krebs-Ringer solution at 37°C, which was maintained throughout the experiment, and permanently oxygenated with a mixture of 95% oxygen and 5% carbon dioxide. The Krebs-Ringer solution was composed as follows (mM): NaCl (119), KCl (5), $MgCl_2 \cdot 6H_2O$ (1.2), $NaHCO_3$ (25), $NaH_2PO_4 \cdot H_2O$ (0.4), $Na_2HPO_4 \cdot 7H_2O$ (1.6), $CaCl_2$ (1.2), and D-glucose (10). The short circuit current was recorded when the voltage was 0 mV. To evaluate transepithelial electrical resistance, we recorded voltage fluctuations when the current was 10 μA, and calculated it using Ohm's law:

$$R = \Delta U / I \, (\mathrm{Ohm})$$

The size of the examined tissue was calculated by using the diameter of the slotted opening between the two chamber-halves (4 mm), and was equal to 0.13 cm^2. With regard to the size of the examined tissue, we adjusted the obtained transepithelial voltage values for 1 cm^2 of tissue (Ohm·cm^2).

We used an electrophysiological method to study all samples, except for samples of tumor that were >113 mm^2 and did not fit into the Ussing chamber.

Assessment of the paracellular permeability of the intestinal wall

To assess the paracellular permeability of the intestine in the Ussing chamber, we added fluorescein to the mucosal bathing solution at a final concentration of 100 μM. This concentration was determined from earlier published reports[24]. Twenty-five minutes after the experiment started, the serosal bathing solution was removed to assess the concentration of the diffused fluorescein. To assess the optical density of this solution, we used a Cary Eclipse Fluorescence Spectrophotometer (Agilent, USA). The excitation and emission wavelengths were 460 and 515 nm, respectively. The permeability coefficient (P_{app}, cm/s) was calculated using the following equitation:

$$P_{app} = (dQ/dt) / (A \cdot C_0) \text{, where :}$$

dQ/dt is the concentration of fluorescein in the serosal bathing solution (mol/s), A is the size of the examined tissue (cm^2), and C_0 is the concentration of fluorescein in the mucosal bathing solution[25].

We assessed paracellular permeability in 38 control and 41 experimental samples, the latter of which included 14 tumor tissue samples, 18 tumor-adjacent tissue samples, and 9 non-tumor tissue samples. The tumor-adjacent tissues consisted of all the tissues from the tumor-neighboring areas on both sides of the tumors.

Optical microscopy for morphological analysis of the intestinal tissue samples

Once the barrier properties were studied in the Ussing chamber, we observed the intestinal samples by optical microscopy. Briefly, the tissue samples were fixed in 10% neutral buffered formalin and histologically processed for embedding in paraffin to prepare ~5 μm-thick tissue sections, which were examined by H&E staining and under a Leica DM IL LED Fluor Inverted Fluorescent Microscope.

Statistical analysis

The data were analyzed using Student's *t*-test and Mann-Whitney *U*-test. The results of the analysis are presented as mean ± standard error (M ± SE). Statistically reliable differences were reported with a probability value of 95% ($P < 0.05$).

Results

The body weights study

The body weights of both the control and experimental animals increased similarly and were (400 ± 15.3) g and (382 ± 16.3) g, respectively, at 6 months after the experiment started.

Morphometric and histological studies

Six months after the experiment started, no tumor was found in the control rats ($n = 8$). The thicknesses of the intact large intestinal wall in the fold areas of the ascending and descending colon were 400–1200 μm and 850 μm, respectively (**Figure 2A**, **B**). All rats injected with DMH ($n = 10$) developed colon tumors, primarily in the descending colon (**Table 1**). The tumor incidence rates varied in different parts of the colon parts, and were 20% in the ascending colon, 90%

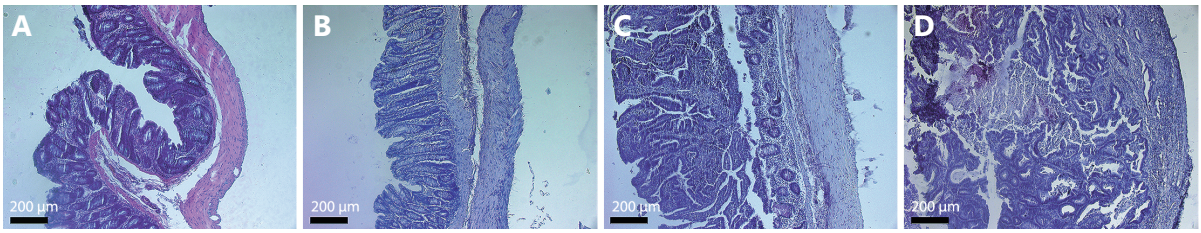

Figure 2 Microphotographs of cross-section of the large intestine wall. (A) Normal ascending colon wall. (B) Normal descending colon wall. (C, D) 1,2-dimethylhydrazine-induced colon adenocarcinomas in the descending colon (H&E staining, scale bar 200 μm).

Table 1 Colon tumor localization, incidence, multiplicity and size in rats exposed to DMH

Parameters	
No. of rats	10
Total colon	
No. of tumor-bearing rats	10 (100%)
No. of tumors	25
No. of tumors per tumor-bearing rat	2.5
Mean size of tumors, mm^2	61±12.8
Ascending colon	
No. of tumor-bearing rats	2 (20%)
No. of tumors	3 (12%)
No. of tumors per tumor-bearing rat	1.5
Mean size of tumors, mm^2	89±37.8
Transverse colon	
No. of tumor-bearing rats	1 (10%)
No. of tumors	1 (4%)
No. of tumors per tumor-bearing rat	1
Size of the tumor, mm^2	27
Descending colon	
No. of tumor-bearing rats	9 (90%)
No. of tumors	17 (68%)
No. of tumors per tumor-bearing rat	2
Mean size of tumors, mm^2	56±14.4
Rectum	
No. of tumor-bearing rats	4 (40%)
No. of tumors	4 (16%)
No. of tumors per tumor-bearing rat	1
Mean size of tumors, mm^2	70±75.9

in the descending colon, and 30% in the rectum. Moreover, 76% of the colon tumors were in the descending colon, 12% were in the ascending colon, and 12% were in the rectum.

Macroscopically, neoplasms are exophytic or endophytic. Microscopically, there are different types of malignant intestinal tumors, and among these, tubular adenocarcinomas are predominant. All carcinoma types are typical in DMH-induced neoplasms[26]. The thickness of the intestinal wall with tumors was 1300–3000 μm (**Figure 2C, D**).

The electrophysiological study

The study showed that the short circuit current and transepithelial electrical resistance of the segments of the ascending colon differed from those of most segments of the descending colon in control rats (**Figure 3A, B**). The short-circuit current in the proximal segment of the ascending colon did not differ from the other segments of the same region but was significantly higher than those of most segments of the descending colon. The transepithelial electrical resistance of the b segment of the ascending colon was significantly higher than that of most segments of the descending colon.

The short circuit current in the tumor tissues of rats injected with DMH was relatively lower, while the transepithelial electric resistance was roughly 4 times higher than that of other non-tumor intestinal segments and segments from the control group (**Figure 4**).

Study of paracellular permeability to fluorescein

No statistically reliable differences in paracellular permeability were found among intestinal segments in the control group (Mann-Whitney U-test; **Figure 4C**).

Examination of the spectral density of the fluorescein solutions revealed statistically reliable evidence of increased permeability in the tumor-adjacent segments when compared to the control group (**Figure 5**). Unlike the control group, in each experimental rat, we found 1–3 segments that

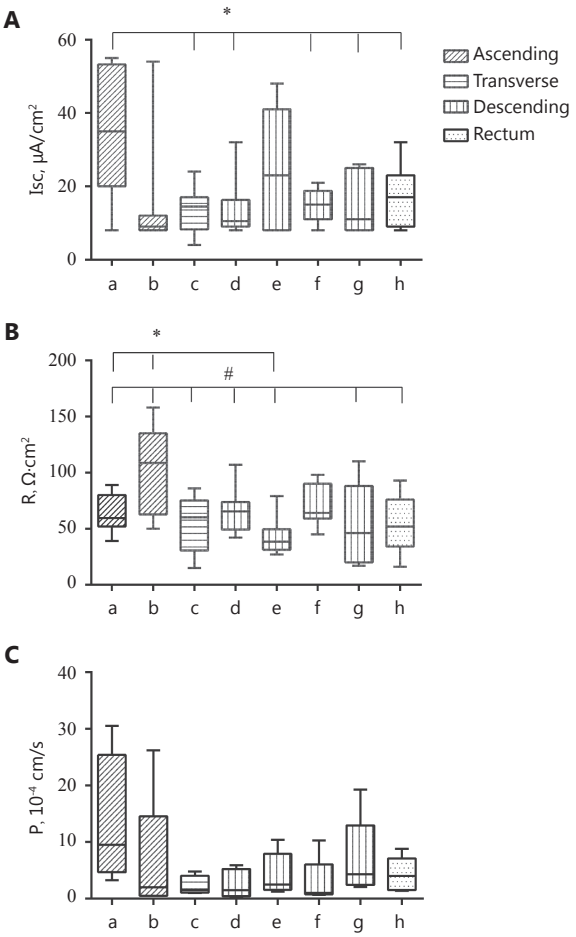

Figure 3 Permeability parameters in rats from the control group. (A) Short circuit current. (B) Transepithelial electric resistance. (C) Permeability for fluorescein in the segments of the (a, b) ascending. (c) Transverse, (d-g) descending parts of the colon, and (h) the rectum. (A) **P* < 0.05, the (a) segment compared with the marked segments, (B) **P* < 0.05, the (a) segment compared with the marked segments, #*P* < 0.05, the (b) segment compared with the marked segments, Student's *t*-test ($n_{\text{all control}}$=62, n_a=8, n_b=8, n_c=8, n_d=8, n_e=8, n_f=8, n_g=7, n_h=7), (C) no significant differences, Mann-Whitney *U*-test (n_{control}=38: n_a=4, n_b=5, n_c=4, n_d=5, n_e=5, n_f=5, n_g=5, n_h=5).

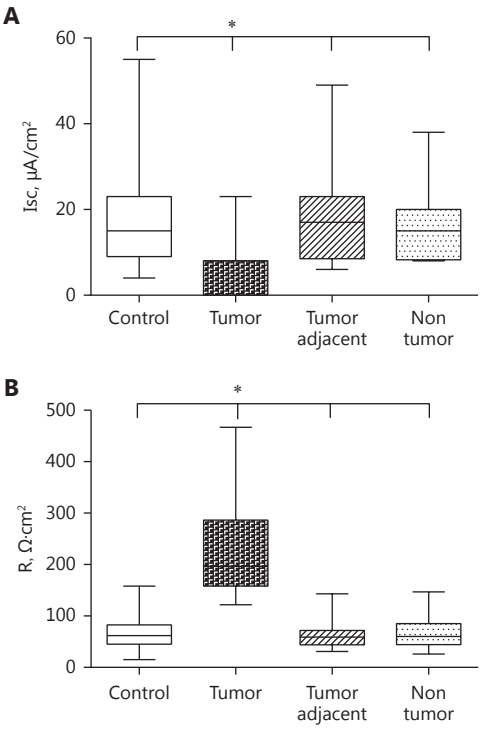

Figure 4 Electrophysiological parameters in the intestinal segments in rats from the experimental group compared with the control group. (A) Short circuit current. (B) Transepithelial electrical resistance. **P* < 0.0001 compared with the control group and other segments, Student's *t*-test (n_{control}=62, n_{tumor}=16, $n_{\text{tumor-adjacent}}$=27, $n_{\text{non-tumor}}$=29).

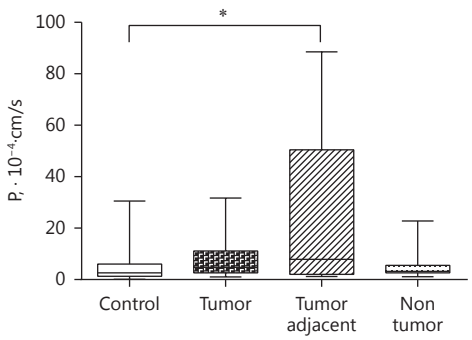

Figure 5 Permeability for fluorescein in the intestinal segments in rats from the experimental group compared with the control group. **P* < 0.01 compared with the control group, Mann-Whitney *U*-test (n_{control}=38, n_{tumor}=9, $n_{\text{tumor-adjacent}}$=18, $n_{\text{non-tumor}}$=14).

had considerably increased permeability (**Figure 6**). The percentage of tumor-adjacent segments that had increased permeability was 44%.

Discussion

In DMH-induced colon tumor adenocarcinoma, the tumors tend to develop *de novo* and are not caused by the inflammatory processes that are typically associated with increased intestinal permeability and often considered to be a probable cause of CRC[5,27]. DMH induces DNA methylation of stem colonocytes located at the base of the crypts of Lieberkühn and subsequent development adenocarcinoma predominantly in the descending colon[17,28]. This

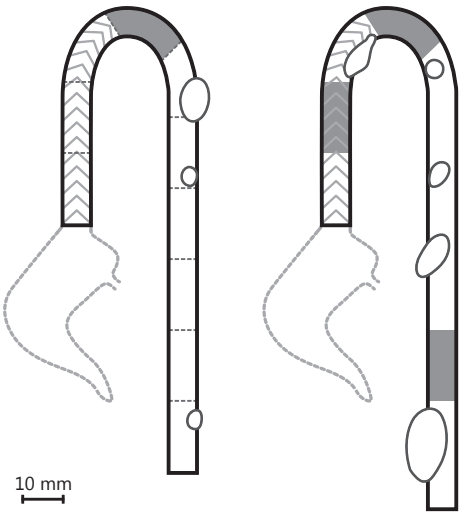

Figure 6 Two examples of localization of the tumors and segments that have increased paracellular permeability (highlighted grey) in the colon in experimental rats (scheme).

experimental model can be regarded as an adequate model for CRC in humans as it incorporates the morphological, genetic, and biochemical aspects of its pathogenesis[28-31], and thus allows us to study how carcinogenesis is directly associated with intestinal permeability, rather than proceeding through inflammation.

Permeability is related to trans- and paracellular permeability to the ions and macromolecules that are actively or passively transported through the mucosal epithelium, which has well-marked barrier properties, and also through the submucosa, muscular layer, and serosa. The electrophysiological properties, i.e., short circuit current and transepithelial electrical resistance, reflect the transport of ions through the intestinal wall, in particular Na^+ and other charged particles. Permeability to macromolecules, such as fluorescein in our experiment, is associated with paracellular permeability, which is related to the epithelial tight junctions[32].

Our research showed that the electrophysiological properties of the ascending and descending colon were not the same. In particular, the transepithelial electrical resistance of one segment of the ascending colon was significantly higher than that of most other segments. These differences could be due to the folds in the ascending colon and the peculiarity of the relief of the proximal colon. As a result, tissue samples of the ascending colon had a larger surface area than samples of the descending colon. However, the heterogeneity in the proximal and distal colon may have contributed to the observed results. Ion transport, i.e., Na^+ absorption, in the proximal and distal colon depends on different mechanisms[1,18]. In the proximal colon, Na^+ movement occurs via electroneutral Na^+ absorption, while in the distal colon, that is mostly associated with amiloride-sensitive and aldosterone-regulated sodium channels, and Na^+ is absorbed mostly through electrogenic transport[33,34]. In rats, Na^+ movement is associated with electroneutral Na^+ absorption[33-35]. Our research findings showed that comparative study of different parts of the colon requires precise measurement of the surface area of the tissue samples and the use of a calculated correction factor. Therefore, this subject requires further study.

The electrophysiological study of the intestinal wall in the rats injected with DMH showed changes in the permeability of the tumor tissues but did not reveal any significant changes in the permeability of other segments in comparison to that of the control group. The increased transepithelial electric resistance in the areas of neoplasm development indicated decreased intestinal permeability.

Moreover, our experiment shows that paracellular permeability to fluorescein in the tumor tissues was the same as that in the control group tissues; thus, it did not contribute to the overall intestinal permeability.

Presumably, the decreased short circuit current and increased transepithelial electrical resistance in the areas of neoplasm development are related to the intestinal wall thickening, as the tumor tissue samples were 1.5 to 3.5 times thicker than the control tissues (**Figure 6**). The decreased intestinal permeability in the tumor tissues could be associated with the decreased intensity of active transport through the tumor tissues of the intestinal wall.

DMH, as some authors argue, can destroy the conductivity of epithelial electrogenic sodium channels and may directly influence the transepithelial potentials in the intestine of rats at the earliest stages of colon carcinogenesis, when no morphological signs are visible and the tumor has not yet developed[36-38]. However, similar changes in the properties and processes of ion transport have been observed in HT-29 and T84 colon carcinoma cells, when calcium-activated chloride secretion is not induced and sodium reabsorption does not occur, which is unlike normal cells[1]. Presumably, the changes in the electrophysiological properties of the tumor tissues we observed in our experiment are associated with decreased differentiation of the tumor cells, resulting from DMH injection and consequent ion transport disruption.

Presumably, the low permeability of the tumors was due to changes in the expression of tight junction proteins, as studies suggest, the expression of claudin 1, 3, and 4, which

decrease epithelial permeability, is enhanced in tumors[8].Our research findings contradict those obtained by Soler et al.[7], who studied biopsy material from human colon tumors and separated intestinal mucosa of rats injected with DMH. By measuring the transepithelial electrical resistance and paracellular flux rate of D-[^{14}C]mannitol they showed that the epithelium of the DMH-induced tumors in rat colon was leakier than the epithelium of normal rat colon.

As the electrophysiological properties of the separated intestinal mucosa and those of intestinal wall with the mucosa, subepithelial muscular layer, and serosa are nearly the same[39,40], the difference we observed in our study can be accounted for by other reasons, for example, differences in sample preparation or other experimental conditions.

Our research findings showed that the paracellular permeability to fluorescein of the tumor tissues did not differ from that the control group, and it is considerably increased in 44% of the tumor-adjacent segments of the colon.

Our scheme to map the intestine allowed us to carry out a painstaking study of intestinal permeability to determine which segments are characterized by increased paracellular in each experimental rat. Destruction of the barrier properties in tumor-adjacent segments of the intestine could be caused by the physical or chemical factors that are associated with cancer. Among them is tumor-induced pressure on adjacent tissues[41], increased enzyme activity and NO production[42-45], active forms of oxygen[46-49], and proinflammatory cytokines[11-13]. Increased paracellular permeability is primarily caused by interleukin-1β (IL-1β), TNF-α, and interferon gamma (IFNγ)[44,50-52], which are produced by both activated immunocompetent cells and tumor cells. As the cytokines are produced, the tumors transform the local cytokine status to one that is more pronounced and aggressive for progressing tumors[11,53].

The properties of the tumor-adjacent tissues, as some studies suggest, are different from those of control tissues. Moreover, tumor-adjacent tissues tend to have cancer-like properties. In particular, studies suggest that tumor-adjacent tissues are characterized by increased paracellular permeability to mannitol[7], changes in enzyme activity[13], increased DNA methylation[13,54], increased expression of genes that produce inflammatory mediators, activate leukocytes, and regulate their mobility, regulate the proliferation of monocytes, and produce interferons[55]. According to these experimental data, the tumor-adjacent tissues of the intestinal wall, which show no signs of morphological changes, can have morpho-functional changes at the subcellular and molecular levels. Therefore, these tissues are inappropriate for use as controls in tumor studies, although this approach is used in some studies[56-58].

In summary, our study showed that the tumor tissues of the intestinal wall have decreased intestinal permeability, while the tumor-adjacent tissues have increased paracellular permeability, without any change in electrophysiological properties. Studies have shown that paracellular permeability to macromolecules can be increased without changing ion permeability[59] or affecting transepithelial resistance[60,61]. Increased paracellular permeability to macromolecules of tumor-adjacent tissues indicates that tumors can negatively influence tumor-adjacent tissues. How this process occurs on a molecular level is another step in the diagnosis and treatment of CRC.

Acknowledgments

This work was supported by a grant from the St. Petersburg State University (Grant No. 1.40.486.2017). Scientific research was performed at the Research park of St. Petersburg State University Center for Molecular and Cell Technologies. We are grateful to Associate Professor Irina A. Lekomtseva, Department of English Philology and Translation, St Petersburg University, for help during translation of this article.

Conflict of interest statement

No potential conflicts of interest are disclosed.

References

1. Kunzelmann K, Mall M. Electrolyte transport in the mammalian colon: mechanisms and implications for disease. Phys Rev. 2002; 82: 245-89.
2. Markov AG, Veshnyakova A, Fromm M, Amasheh M, Amasheh S. Segmental expression of claudin proteins correlates with tight junction barrier properties in rat intestine. J Comp Phys B. 2010; 180: 591-8.
3. Fink MP. Intestinal epithelial hyperpermeability: update on the pathogenesis of gut mucosal barrier dysfunction in critical illness. Curr Opin Crit Care. 2003; 9: 143-51.
4. Landy J, Ronde E, English N, Clark SK, Hart AL, Knight SC, et al. Tight junctions in inflammatory bowel diseases and inflammatory bowel disease associated colorectal cancer. World J Gastroenterol. 2016; 22: 3117-26.
5. Pastorelli L, De Salvo C, Mercado JR, Vecchi M, Pizarro TT. Central role of the gut epithelial barrier in the pathogenesis of chronic intestinal inflammation: lessons learned from animal models and human genetics. Front Immunol. 2013; 4: 280
6. Martin TA, Jiang WG. Tight junctions and their role in cancer

metastasis. Histol Histopathol. 2001; 16: 1183-95.
7. Soler AP, Miller RD, Laughlin KV, Carp NZ, Klurfeld DM, Mullin JM. Increased tight junctional permeability is associated with the development of colon cancer. Carcinogenesis. 1999; 20: 1425-32.
8. Wang XX, Tully O, Ngo B, Zitin M, Mullin JM. Epithelial tight junctional changes in colorectal cancer tissues. ScientificWorldJournal. 2011; 11: 826-41.
9. Singh AB, Sharma A, Dhawan P. Claudin family of proteins and cancer: an overview. J Oncol. 2010; 2010: 541957
10. Ferlay J, Soerjomataram I, Dikshit R, Eser S, Mathers C, Rebelo M, et al. Cancer incidence and mortality worldwide: sources, methods and major patterns in GLOBOCAN 2012. Int J Cancer. 2015; 136: E359-86.
11. Hiribarren A, Heyman M, L'Helgouach A, Desjeux JF. Effect of cytokines on the epithelial function of the human colon carcinoma cell line HT29 cl 19A. Gut. 1993; 34: 616-20.
12. Al-Sadi R, Boivin M, Ma T. Mechanism of cytokine modulation of epithelial tight junction barrier. Front Biosci. 2009; 14: 2765-78.
13. Nusrat A, Turner JR, Madara JL. Molecular physiology and pathophysiology of tight junctions. IV. Regulation of tight junctions by extracellular stimuli: nutrients, cytokines, and immune cells. Am J Physiol Gastrointest Liver Physiol. 2000; 279: G851-7.
14. Bishop WP, Wen JT. Regulation of Caco-2 cell proliferation by basolateral membrane epidermal growth factor receptors. Am J Physiol. 1994; 267: G892-900.
15. Mullin JM, Agostino N, Rendon-Huerta E, Thornton JJ. Keynote review: epithelial and endothelial barriers in human disease. Drug Discov Today. 2005; 10: 395-408.
16. Pozharisski KM. Morphology and morphogenesis of experimental epithelial tumors of the intestine. J Natl Cancer Inst. 1975; 54: 1115-35.
17. Bekusova VV, Patsanovskii VM, Nozdrachev AD, Trashkov AP, Artemenko MR, Anisimov VN. Metformin prevents hormonal and metabolic disturbances and 1, 2-dimethylhydrazine-induced colon carcinogenesis in non-diabetic rats. Cancer Biol Med. 2017; 14: 100-7.
18. Tang LQ, Fang XF, Winesett SP, Cheng CY, Binder HJ, Rivkees SA, et al. Bumetanide increases Cl^--dependent short-circuit current in late distal colon: evidence for the presence of active electrogenic Cl-absorption. PLoS One. 2017; 12: e0171045
19. Mahler M, Berard M, Feinstein R, Gallagher A, Illgen-Wilcke B, Pritchett-Corning K, et al. FELASA recommendations for the health monitoring of mouse, rat, hamster, guinea pig and rabbit colonies in breeding and experimental units. Lab Anim. 2014; 48: 178-92.
20. Pozharisski KM, Shaposhnikov JD, Petrov AS, Likhachev AJ. Distribution and carcinogenic action of 1,2-dimethylhydrazine (SDMH) in rats. Z Krebsforsch Klin Onkol. 1976; 87: 67-80.
21. Pozharisski KM, Likhachev AJ, Shaposhnikov JD, Petrov AS, Balansky RM. Dependence of 1,2-dimethylhydrazine metabolism on its treatment schedule. Cancer Lett. 1977; 2: 185-90.
22. Mullin JM, Laughlin KV, Ginanni N, Marano CW, Clarke HM, Soler AP. Increased tight junction permeability can result from protein kinase C activation/translocation and act as a tumor promotional event in epithelial cancers. Ann N Y Acad Sci. 2000; 915: 231-6.
23. Markov AG, Falchuk EL, Kruglova NM, Radloff J, Amasheh S. Claudin expression in follicle-associated epithelium of rat Peyer's patches defines a major restriction of the paracellular pathway. Acta Physiol. 2016; 216: 112-9.
24. Molenda N, Urbanova K, Weiser N, Kusche-Vihrog K, Günzel D, Schillers H. Paracellular transport through healthy and cystic fibrosis bronchial epithelial cell lines - do we have a proper model? PLoS One. 2014; 9: e100621
25. Žakelj S, Legen I, Veber M, Kristl A. The influence of buffer composition on tissue integrity during permeability experiments "in vitro". Int J Pharm. 2004; 272: 173-80.
26. Turusov VS. Nomenclature and histological classification of tumors in laboratory-animals. Eksp Onkol. 1992; 14: 8-13.
27. Du LJ, Kim JJ, Shen JH, Dai N. Crosstalk between inflammation and ROCK/MLCK signaling pathways in gastrointestinal disorders with intestinal hyperpermeability. Gastroenterol Res Pract. 2016; 2016: 7374197
28. Pozharisski KM, Kapustin YM, Likhachev AJ, Shaposhnikov JD. The mechanism of carcinogenic action of 1,2-dimethylhydrazine (SDMH) in rats. Int J Cancer. 1975; 15: 673-83.
29. Perse M, Cerar A. Dimethylhydrazine model is not appropriate for evaluating effect of ethanol on colorectal cancer. Rev Esp Enferm Dig. 2007; 99: 463-6.
30. Washington MK, Powell AE, Sullivan R, Sundberg JP, Wright N, Coffey RJ, et al. Pathology of rodent models of intestinal cancer: progress report and recommendations. Gastroenterology. 2013; 144: 705-17.
31. Perše M, Cerar A. Morphological and molecular alterations in 1,2 dimethylhydrazine and azoxymethane induced colon carcinogenesis in rats. J Biomed Biotechnol. 2011; 2011: 473964
32. Krug SM, Schulzke JD, Fromm M. Tight junction, selective permeability, and related diseases. Semin Cell Dev Biol. 2014; 36: 166-76.
33. Yau WM, Makhlouf GM. Comparison of transport mechanisms in isolated ascending and descending rat colon. Am J Physiol. 1975; 228: 191-5.
34. Sandle GI, Wills NK, Alles W, Binder HJ. Electrophysiology of the human colon: evidence of segmental heterogeneity. Gut. 1986; 27: 999-1005.
35. Binder HJ, Foster ES, Budinger ME, Hayslett JP. Mechanism of electroneutral sodium chloride absorption in distal colon of the rat. Gastroenterology. 1987; 93: 449-55.
36. Fraser GM, Portnoy M, Bleich M, Ecke D, Niv Y, Greger R, et al. Characterization of sodium and chloride conductances in preneoplastic and neoplastic murine colonocytes. Pflugers Arch. 1997; 434: 801-8.
37. Bleich M, Ecke D, Schwartz B, Fraser G, Greger R. Effects of the

carcinogen dimethylhydrazine (DMH) on the function of rat colonic crypts. Pflugers Arch. 1997; 433: 254-9.
38. Davies RJ, Asbun H, Thompson SM, Goller DA, Sandle GI. Uncoupling of sodium chloride transport in premalignant mouse colon. Gastroenterology. 1990; 98: 1502-8.
39. Gitter AH, Fromm M, Schulzke JD. Impedance analysis for the determination of epithelial and subepithelial resistance in intestinal tissues. J Biochem Biophys Methods. 1998; 37: 35-46.
40. Markov AG, Amasheh S. Barrier properties and tight junction protein expression along the longitudinal axis of rat intestine. Ross Fiziol Zh Im I M Sechenova. 2011; 97: 1066-83.
41. Miessler KS, Vitzthum C, Markov AG, Amasheh S. Effects of basal hydrostatic pressure on differentiated and undifferentiated mammary epithelial cells. Acta Physiologica. 2017; 219: 90
42. Unno N, Menconi MJ, Smith M, Aguirre DE, Fink MP. Hyperpermeability of intestinal epithelial monolayers is induced by NO: effect of low extracellular pH. Am J Physiol. 1997; 272: G923-34.
43. Unno N, Fink MP. INTESTINAL EPITHELIAL HYPERPERMEABILITY: mechanisms and relevance to disease. Gastroenterol Clin North Am. 1998; 27: 289-307.
44. Chavez AM, Menconi MJ, Hodin RA, Fink MP. Cytokine-induced intestinal epithelial hyperpermeability: role of nitric oxide. Crit Care Med. 1999; 27: 2246-51.
45. Ng CT, Fong LY, Low YY, Ban J, Hakim MN, Ahmad Z. Nitric oxide participates in IFN-γ-induced HUVECs hyperpermeability. Physiol Res. 2016; 65: 1053-8.
46. Banan A, Fields JZ, Farhadi A, Talmage DA, Zhang L, Keshavarzian A. Activation of δ-isoform of protein kinase C is required for oxidant-induced disruption of both the microtubule cytoskeleton and permeability barrier of intestinal epithelia. J Pharmacol Exp Ther. 2002; 303: 17-28.
47. Gonzalez PK, Doctrow SR, Malfroy B, Fink MP. Role of oxidant stress and iron delocalization in acidosis-induced intestinal epithelial hyperpermeability. Shock. 1997; 8: 108-14.
48. Wang N, Han Q, Wang G, Ma WP, Wang J, Wu WX, et al. Resveratrol protects oxidative stress-induced intestinal epithelial barrier dysfunction by upregulating heme oxygenase-1 expression. Dig Dis Sci. 2016; 61: 2522-34.
49. Perše M. Oxidative stress in the pathogenesis of colorectal cancer: cause or consequence? BioMed Res Int. 2013; 2013: 725710
50. He F, Peng J, Deng XL, Yang LF, Camara AD, Omran A, et al. Mechanisms of tumor necrosis factor-alpha-induced leaks in intestine epithelial barrier. Cytokine. 2012; 59: 264-72.
51. Freour T, Jarry A, Bach-Ngohou K, Dejoie T, Bou-Hanna C, Denis MG, et al. TACE inhibition amplifies TNF-alpha-mediated colonic epithelial barrier disruption. Int J Mol Med. 2009; 23: 41-8.
52. Unno N, Hodin RA, Fink MP. Acidic conditions exacerbate interferon-gamma-induced intestinal epithelial hyperpermeability: role of peroxynitrous acid. Crit Care Med. 1999; 27: 1429-36.
53. Lee JS, Tato CM, Joyce-Shaikh B, Gulen MF, Cayatte C, Chen Y, et al. Interleukin-23-independent IL-17 production regulates intestinal epithelial permeability. Immunity. 2015; 43: 727-38.
54. Richiardi L, Fiano V, Grasso C, Zugna D, Delsedime L, Gillio-Tos A, et al. Methylation of APC and GSTP1 in non-neoplastic tissue adjacent to prostate tumour and mortality from prostate cancer. PLoS One. 2013; 8: e68162
55. Casbas-Hernandez P, Sun XZ, Roman-Perez E, D'Arcy M, Sandhu R, Hishida A, et al. Tumor intrinsic subtype is reflected in cancer-adjacent tissue. Cancer Epidemiol Biomarkers Prev. 2015; 24: 406-14.
56. Miwa N, Furuse M, Tsukita S, Niikawa N, Nakamura Y, Furukawa Y. Involvement of claudin-1 in the beta-β/Tcf signaling pathway and its frequent upregulation in human colorectal cancers. Oncol Res. 2001; 12: 469-76.
57. Gröne J, Weber B, Staub E, Heinze M, Klaman I, Pilarsky C, et al. Differential expression of genes encoding tight junction proteins in colorectal cancer: frequent dysregulation of claudin-1, -8 and -12. Int J Colorectal Dis. 2007; 22: 651-9.
58. Kimura Y, Shiozaki H, Hirao M, Maeno Y, Doki Y, Inoue M, et al. Expression of occludin, tight-junction-associated protein, in human digestive tract. Am J Pathol. 1997; 151: 45-54.
59. Krug SM, Amasheh S, Richter JF, Milatz S, Gunzel D, Westphal JK, et al. Tricellulin forms a barrier to macromolecules in tricellular tight junctions without affecting ion permeability. Mol Biol Cell. 2009; 20: 3713724
60. Al-Sadi R, Khatib K, Guo SH, Ye DM, Youssef M, Ma T. Occludin regulates macromolecule flux across the intestinal epithelial tight junction barrier. Am J Physiol Gastrointest Liver Physiol. 2011; 300: G1054-64.
61. Balda MS, Whitney JA, Flores C, González S, Cereijido M, Matter K. Functional dissociation of paracellular permeability and transepithelial electrical resistance and disruption of the apical-basolateral intramembrane diffusion barrier by expression of a mutant tight junction membrane protein. J Cell Biol. 1996; 134: 1031-49.

Cite this article as: Bekusova VV, Falchuk EL, Okorokova LS, Kruglova NM, Nozdrachev tumor-adjacent areas in 1,2-dimethylhydrazine-induced colon carcinogenesis in rats. Cancer Biol Med. 2018; 15: 251-9. doi: 10.20892/j.issn.2095-3941.2018.0016